Determination of absorption of thermal radiation by black and silvery body surfaces

Article · February 2021

3 authors, including:

Otor Daniel Abi
University of Agriculture
11 PUBLICATIONS   18 CITATIONS

SEE PROFILE

Determination of absorption of thermal radiation by black and silvery body surfaces

Otor D.A.[*]**, Ikyo D.A. and Ogwuche I.E.**
Department of Physics, College of Science, University of Agriculture, Makurdi, Benue State, Nigeria
otordanabi@gmail.com

Abstract

Absorption of radiation by black surfaces and silvery surfaces was carried out using several material samples of black and silvery surfaces/liquids. An investigation of our material samples using temperature sensors reveals that sharp increase in radiation are more pronounced on black surfaces/liquids than that of silvery surfaces/liquids. The geometrical configuration was greatly altered as the power radiated from rear surfaces were measured by sensors as different material samples are taken into account with respect to time. We investigated theoretically that for an evacuated container, the thermal energy transfer is solely due to radiation as the vacuum is kept between two spheres while for a non-evacuated container, an extra heat transfer occurs due to the air's thermal conductance if the spheres separation contains air. The temperature distribution in presence of heat sources was calculated and the results are in good agreement with the experimental results. The results of rate of absorption of radiation by the black surfaces and silvery surfaces for different material samples were compared. These results reveal that black surfaces absorb radiation at greater rate as compared to silvery surfaces with respect to time. We recommend that other colors apart from black and silvery be used or added as material samples in further research work.

Keywords: Black body surface, Silvery body surface, Temperature Distribution and Thermal Radiation.

Introduction

One of the most important applications of quantum statistics for bosons is the description of the electromagnetic radiation that is photon gas in thermal equilibrium[1]. This radiation is usually called the blackbody radiation. Maxwell's equations describing electromagnetic field dynamic equations are nonlinear equations[2], which imply that there are no interactions between photons in media that can be modelled by non-linear electric field[3], e.g. in vacuum.

The absorption of radiation by a black body surface and a silvery surface are undoubtedly one of the most significant aspects that determined the rate of absorption and reflection of temperature[4]. The rate at which a body absorbs radiation depends upon the nature of the surface, objects that are good emitters are also good absorbers, In general shiny coloured (eg silvery) and metallic surfaces emit or absorb radiation energy slowly since they reflects radiation, dark coloured (e.g. black) surfaces emit or absorb radiation energy more effectively[5].

Ionize radiation can travel through a vacuum when the ionized radiation hits an object[6]. Some of the energy is absorbed making the object temperature to increase and some are reflected making the object temperature to reduce and the rate at which a surface absorbed or reflected radiation is largely determined by the colour of the object surface and it greatly affect the temperature of an object[7].

Transmission of energy in form of waves or particles through space or through a material medium[8], that include electromagnetic radiation such as radio waves, microwaves, infrared, visible light, ultraviolet, x-ray and gamma radiation are evidence of Radiation. It can be noted that Particle radiation such as alpha radiation, beta radiation and neuron radiation are non-zero rest energy[9], acoustic radiation such as ultrasound and seismic wave depend on a physical transmission medium[10], and gravitational radiation takes the form of gravitational wave or ripples in the curvature of space time[11].

A brand-new type of spectrum curve of black body thermal radiation is given after studying the normalized Planck's equations in depth with two important parameters, namely relative width RW_η and relative symmetry factor RSF_η[12]. The experimental verification of the parameters use here have three significant; giving a method to measure temperature by detecting the radiation wavelength, determining the blackbody grade and the use of temperature obtained from the law of the blackbody thermal radiation as a criterion.

Under the development of the remote sensing[13], night vision[14], and thermal radiation thermometry technology[15], many further studies on the blackbody thermal radiation have been carried out. For examples, by studying the inflection point feature along the both sides of the curves, the light wave equation of the inflection point was obtained[16].

Thermal properties of groundnut shell were successfully optimized and characterized using Leeds Apparatus and calorimetry[17]. It was observed that the thermal radiation of groundnut shell reinforced polymer composite (GSPC) decreased (0.355–0.221W/mK) with increasing weight percentage (wt%) of the groundnut fiber (GF); while the thermal resistivity increases. Thermal diffusivity decreases with additional particles content.

From the literature surveyed so far, the emphasis was laid mostly on emissivity. Very little or no attention was made towards absorptivity of black and silvery colored surfaces. Based on the aforementioned reasons we shall in this work obtain theoretically the temperature distribution for slab with distributed heat source, investigate the absorption of radiation by a black surface and a slivery surface using different materials with respect to temperature time scaling.

This paper is organized as follows: Theory of Black Body Radiation, Orthogonal Geometry of Ceramic Oven, and Spherical Geometry of Two Concentric Sphere are presented in second heading. The Temperature distribution in presence of heat sources is also presented in this section. Materials and methods are presented in third heading. Results and detailed discussions are given in fourth heading. Summary and conclusion are presented in fifth heading.

Basic Theory: Theory of Black Body Radiation: A black body is an ideal object whose property is to absorb all incident thermal radiation, independently of their wavelength. Likewise, it is also the best radiation emitter; its spectrum is continuous, and for a given temperature, nobody will emit a more intense radiation. A real body whose emitted spectrum is continuous, but whose radiation intensity is lower than expected, is called a grey body[18]. Towards the end of the 21st century, Rayleigh and Jeans studied the theoretical black body, using classical statistical physics as their basis. Their results lead to the following relationship between the energy density and the emitted frequency –

$$U_{RJ}(v) = \frac{8\pi kT}{c^3} v^2 \qquad (1)$$

where U is the energy density, T the black body's temeperature, c the speed of light, k the Boltzmann constant and v the frequency. However, the experimental result, $U_{exp}(v)$ did not follow this equation as shown by Rayleigh and Jeans' calculations, (U_{RJ}) and the measured energy density (U_{exp}). In particular, $v \to \infty$ yields $U_{exp} \to 0$, but $U_{RJ} \to \infty$. This was called the "ultraviolet catastrophe". Planck repeated the study of black body radiation, with the added hypothesis that the energy of the emitted or absorbed radiation of frequency v is quantized, and equal to $E = hv$ where $h = 6.625 \times 10^{-34} J.s$ is Planck's constant. This leads to the following black body spectral distribution: $U(v) = \frac{8\pi h}{c^3} \frac{v^3}{e^{hv/kT}-1}$ or rather expressed as a function of the wavelength $\lambda = c/v$ as shown in Figure-1[6,10,11].

$$U(v) = \frac{8\pi hc}{\lambda^5} \frac{1}{e^{hv/kT}-1} \qquad (2)$$
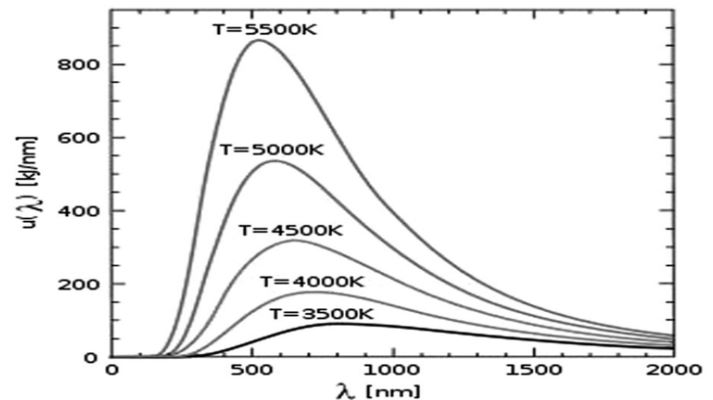

Figure-1: The Original Spectrum Curve of the Blackbody Radiation.

which corresponds perfectly to the experimental value. Integrating this expression over all wavelengths yields a radiated power per unit surface of the body P_N given by:

$$P_N = \frac{2\pi^5 k^4}{15h^3 c^2} . T^4 = \sigma . T^4 \, in \, w/m^2 \qquad (3)$$

where T is the temperature of the emitting surface in Kelvin. Equation (3) is called Stefan-Boltzmann law. It can be note that the Stefan-Boltzmann constant, depends only on three physical constants k, h and c, is equal to:

$$\sigma = 5.67 \times 10^{-8} \, w/m^2 . K^4 \qquad (4)$$

Orthogonal Geometry of Ceramic Oven: Power emitted by the rear surface of a ceramic oven can be calculated considering the fact that the geometric configuration can greatly alter the measurements of the temperature sensors. If the radiation detector that is exactly aligned with the oven gives the half space defined by the emitting surface and the surface of the detector then the oven's emitted power equals $P_{Four} = S_2 \sigma T^4$. The power emitted by the oven (at a temperature T) that is received by the detector is contained in the solid angle Ω_2, so:

$$P_{Four \to Det} = \frac{\Omega_2}{2\pi} S_2 \sigma T^4 \qquad (5)$$

Using an analogous reasoning, we find that the power radiated from the detector (at a temperature T_0) to the oven $P_{Four \to Det}$ is contained in the solid angle Ω_1

$$P_{Four \to Det} = \frac{\Omega_1}{2\pi} S_1 \sigma T^4 \qquad (6)$$

In addition to that, surface S_1 (detector) receives radiation from objects and walls at temperature T_0 in the half space $x > 0$. Out of the solid angle Ω_1: $P_{Obj \to Det}$ and the lamps and people around the object, P_{Obj}. On the other hand, surface S_1 also emits

radiation to all surrounding objects with $x > 0$, out of the solid angle Ω_1: $P_{Obj \to Det}$. Considering all bodies to be black bodies, and since the walls and objects are all at room temperature, T_0, we can state $P_{Obj \to Det} = P_{Det \to Obj}$. We are left with,

$$P_{Total} = P_{Four \to Det} + P_{Obj} - P_{Det \to Four} \qquad (7)$$

Finally, we define the solid angles as

$$\Omega_1 = \frac{S_2}{x_2^2} = \frac{S_d}{x_d^2} \qquad (8)$$

$$\Omega_2 = \frac{S_1}{x_2^2} \Rightarrow \Omega_1 S_1 = \Omega_2 S_2 \qquad (9)$$

Equations (8) and (9) yields:

$$P_{Total} = \frac{S_1 S_d}{2\pi x_d^2} \sigma (T^4 - T_0^4) + P_{Obj} \qquad (10)$$

The detector converts the received power P_{Total} in a voltage V_T, according to a conversion factor C_{Det} such that $V_T = C_{Det} . P_{Total}$ i.e.:

$$V_T = C_{Det} . P_{Total} = C_{Det} . \frac{S_1 S_d}{2\pi x_d^2} \sigma (T^4 - T_0^4) + V_{Obj} \qquad (11)$$

Where $V_{Obj} = C_{Det} P_{Obj}$ offset due to lamps and people. S_1 is the surface of the detector, S_d is the surface of diaphragm opening, x_d is diaphragm-detector distance, C is detector conversion factor, T is Oven's temperature and T_0 is room temperature

Spherical Geometry of Two Concentric Sphere: For two concentric opaque sphere, of surface S and S_0, and temperature T_0 and T, with average absorption factors A_0 and A close to one end, we obtain the effective radiated power as

$$P_T^{emit} = P_{in \to ext}^{emit} - P_{in \to ext}^{reflect} - AP_{ext \to in}^{emit} = AA_0 S \sigma (T^4 - T_0^4) \qquad (12)$$

Since outer sphere is kept in a thermal reservoir (water basin), so T_0 is constant while the inner sphere (Filled with water) is at a slightly higher temperature T with $T = T_0 + \theta$, with $\theta \ll T_0$. Therefore if A_0 and A are known, then measuring the emitted energy as a function of time is enough to determine the Stefan-Boltzmann constant.

For an evacuated container, if a vacuum is kept between both spheres, the thermal energy transfer is solely due to radiation, so the thermal energy variation is given by

$$\kappa \frac{d\theta}{dt} = -P = -\alpha S \sigma (T^4 - T_0^4) \qquad (13)$$

where, $\alpha = AA_0$ and $\kappa = \kappa_{eau} + \kappa_{verre}$ is the heat capacity of internal sphere. Approximating $\theta \ll T_0$, equation (13) becomes (2nd order expansion)

$$\kappa \frac{d\theta}{dt} \approx -\alpha S \sigma \left[4T_0^3 \theta \left(1 + 1.5 \frac{\theta}{T_0} \right) \right] \qquad (14)$$

Introducing the following dimensions:

$$\Phi = \frac{T - T_0}{T_0} = \frac{\theta}{T_0} \quad and \quad \Gamma = \frac{4\alpha T_0^3}{\kappa} \sigma \quad \text{in order to get}$$

$$\frac{d\Phi}{dt} = -\Gamma \Phi (1 + 1.5\Phi) \qquad (15)$$

The solution to this differential equation is

$$In \left(\frac{\Phi}{1 + 1.5\Phi} \right) = -\Gamma t + B \qquad (16)$$

where B is an integration constant defined by $t = 0$.

For a non-evacuated container, If the space separating the spheres contains air rather than a vacuum, and extra heat transfer occurs due to the air's thermal conductance χ. Consequently, equation (13) becomes:

$$\kappa \frac{d\theta}{dt} = -P = -\alpha S \sigma (T^4 - T_0^4) + \chi^\theta \qquad (17)$$

By limiting ourselves to the 1st order expansion of $(T^4 - T_0^4) \approx 4T_0^3 \theta$, we get

$$\frac{d\theta}{dt} = - \left(\Gamma + \frac{\chi}{\kappa} \right) \theta = -\Gamma_{air} \theta$$

Whose solution is given by:

$$\theta(t) = \theta_0 \exp (-\Gamma_{air} t) \qquad (18)$$

Distribution of Temperature around the Sources of Heat: Electrical heaters were electric energy is converted resistively into heat, nuclear power supplier and propellants where chemical energy is the source are number of situations in which there are sources of heat in the domain of interest. These situations shall be analyze by looking at a model problem of a slab with heat source α (W/m^3) distributed throughout. Taking the outside walls to be at temperature T_w, and we will determine the maximum internal temperature.
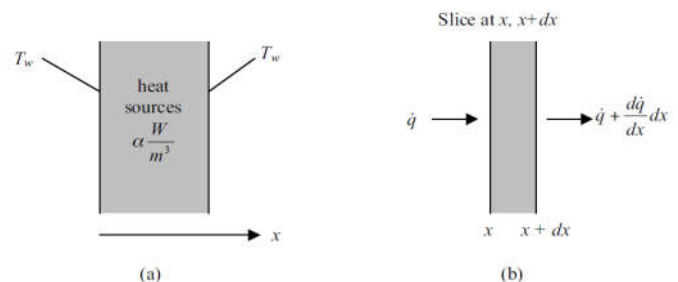

Figure-2: Heat sources from Slab (a) Configured Slab, (b) Elemental Slab.

In Figure-2 (b), an equation for the heat flux, $\dot{q}$ obtained by a steady-state energy balance yields

$$\dot{q} + adx - \left(\dot{q} + \frac{d\dot{q}}{dx}dx\right) = 0$$

or $\frac{d\dot{q}}{dx} = \alpha$

There is a change in heat flux with x due to the presence of heat sources. The equation of temperature can be given by

$$\frac{d^2T}{dx^2} + \frac{\alpha}{k} = 0 \qquad (19)$$

Integrating (19)twice gives

$$T = -\frac{\alpha}{2k}x^2 + ax + b \qquad (20)$$

Were a and b are constants of integration. The boundary conditions imposed are $T(0) = T(L) = T_w$.substituting these into equation (20) gives $b = T_w$ and $a = \frac{\alpha L}{2k}$. The temperature distribution is thus:

$$T = -\frac{\alpha x^2}{2k} + \frac{\alpha}{2k}Lx + T_w \qquad (21)$$

In a normalized form, (21) is a non-dimensional fashion that gives a form that exhibits in a more useful manner the way in which the different parameters enter the problem:

$$\frac{T-T_w}{\alpha L^2/k} = \frac{1}{2}\left(\frac{x}{L} - \frac{x^2}{L^2}\right) \qquad (22)$$

This distribution (Figure-4) is calculated and the results are in good agreement with the experimental results in[19]. About the mid-plane where $x = \frac{L}{2}$, the distribution is symmetric with half the energy due to the sources exiting the slab on each side.

The heat flux at the side of the slab can be found by differentiating the temperature distribution and evaluating$x = 0$; $-k\frac{dT}{dx}\Big|_{x=0} = -k\frac{\alpha L^2}{2K}\left(\frac{1}{L}\right) = -\alpha L/2$. This is half of the total heat generated within the slab. The magnitude of the heat flux is the same at $x = L$ although the direction is opposite.

Again we consider heat flux with boundary conditions at $x = 0$ and $x = L$, so that T_w is not known. We again determine maximum temperature at $x = 0$ and L, by assuming the heat flux and temperature are continuous and so;

$$-k\frac{dT}{dx} = h(T - T_\infty) \qquad \text{at} \quad x = 0, L, \qquad (23)$$

Referring to the temperature distribution of equation (21) gives for the two terms in equation (23),

$$k\frac{dT}{dx} = k\left(-\frac{\alpha x}{k} + a\right) = (-\alpha x + ka) \qquad (24)$$

$$h(T - T_\infty) = h\left(\frac{\alpha x^2}{k} + \alpha x + b - T_\infty\right) \qquad (25)$$

Evaluating (t) at $x = 0$ and L allows determination of the two constant a and b.

Materials and methods

Materials: Two temperature sensors (Thermometers), Data logger, Aluminium (Black and silvery) foils, 100w bulb, Black felt pen, Coal tar, Tick milk, Lamb holder, Black liquor Soap, Watery milk (Shiny), Beaker, Steam generator.

Methods of Solutions: The following procedure described below was used to perform the laboratory experiment: Two temperature sensors were connected to the data logger, one to analog channel A and the other to channel B. The ends of the temperature sensors with aluminium foils of the same dimensions were wrapped. Using a black felt pen, the aluminium foil on the temperature sensor of channel A is blackened while the sensors are at equal distances from the bulb. See the experimental set-up in Figure-3.
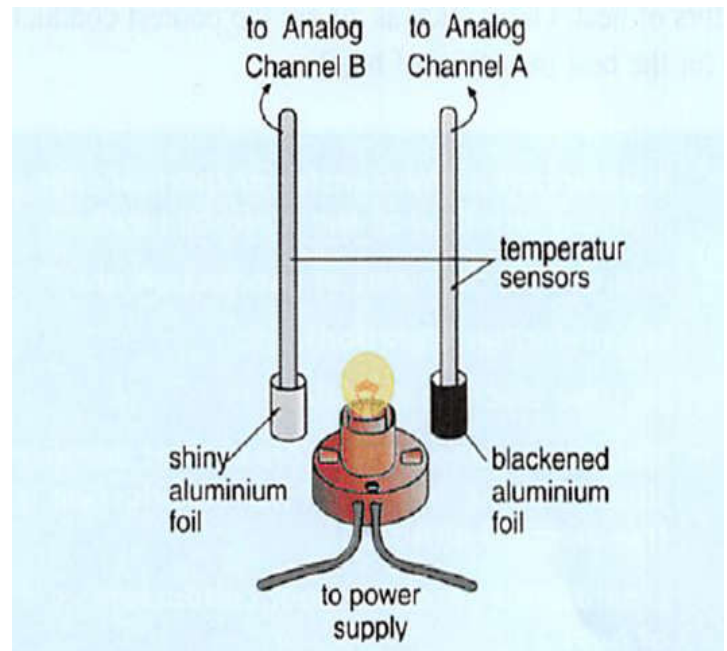

Figure-3: Absorption of Radiation by Black and Shiny Surfaces.

We start the temperature recording by observe the temperature and time, as the bulb was switched on using the temperature sensors as shown in Figure-3. Initial temperatures of both sensors were taking. The bulb was switched off after 60 seconds (one minute) and the temperature readings were taking. The process were repeated using coal tar, tick milk, black liquor soap and watery milk.

Results and Discussions

Table-1: The absorption temperatures of radiation by several black and silvery coloured body surfaces with time.

| Time(Min)	Temperature /°C					
	Al foil black	*Al* foil silvery	Black coal tar	Thick milk	Liquor soap	Watery milk
1.0	35.0	31.0	35.0	31.0	32.0	31.0
2.0	39.0	32.0	39.0	32.0	34.0	32.0
3.0	44.0	33.0	43.0	33.0	36.0	33.0
4.0	47.0	34.0	47.0	34.0	38.0	34.0
5.0	50.0	34.4	50.0	35.0	40.0	35.0
6.0	52.0	34.8	53.0	36.0	42.0	35.4
7.0	53.0	35.2	55.0	37.0	44.0	35.8
8.0	54.0	35.6	57.0	38.0	46.0	36.2
9.0	55.0	36.0	58.0	39.0	48.0	36.7
10.0	56.0	36.2	59.0	39.1	50.0	37.4
11.0	56.4	36.4	60.0	39.2	50.1	37.7
12.0	56.8	36.8	60.5	39.3	50.2	38.1
13.0	57.2	37.0	61.0	39.4	50.3	38.4
14.0	57.4	37.1	61.1	39.5	50.4	38.6
15.0	57.6	37.2	61.1	39.6	50.5	38.8
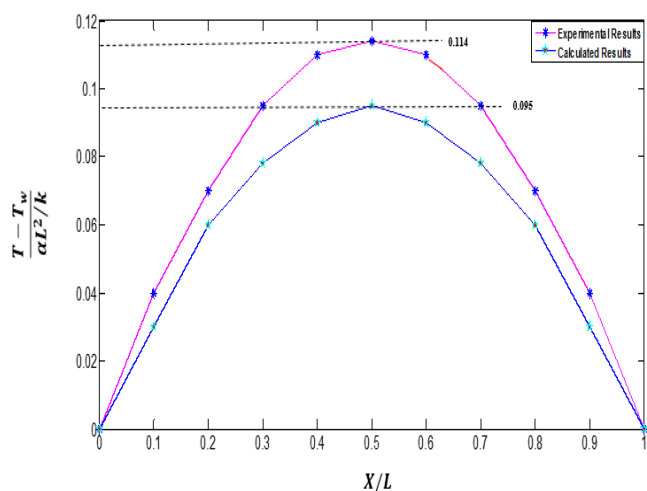
Figure-4: Experimental and Calculated Temperature Distribution for Slab with distributed heat sources.
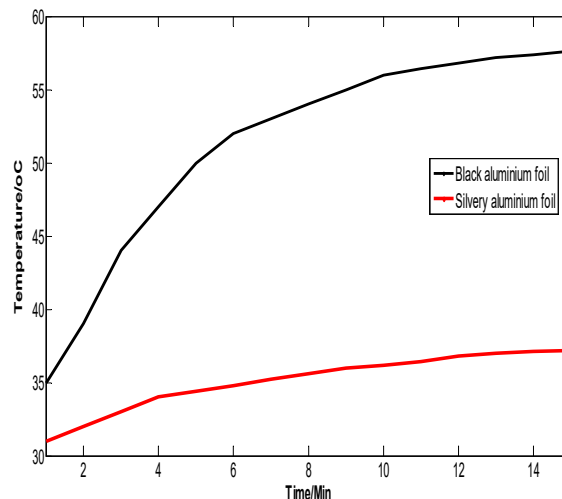

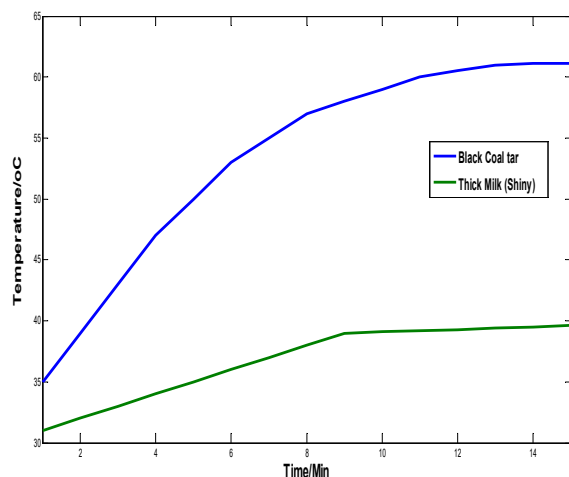**Figure-5:** Temperature-Time graph of Blackened Foil and Silvery Foil.

Figure-6: Temperature-Time graph of Black coal tar and Thick shiny milk.
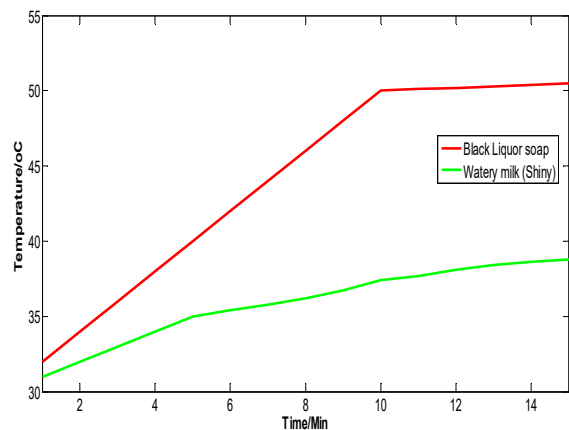

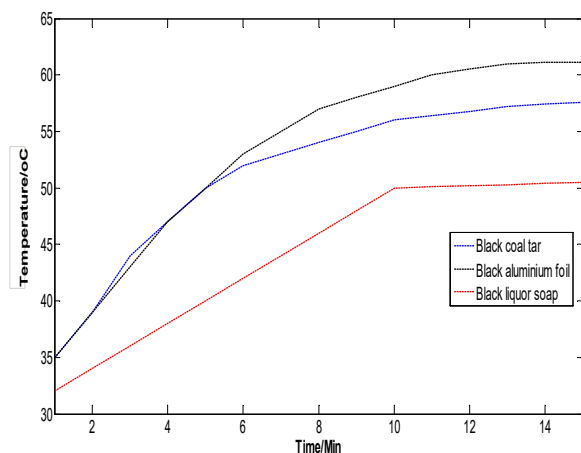**Figure-7:** Temperature-Time graph of Black liquor soap and shiny water milk.

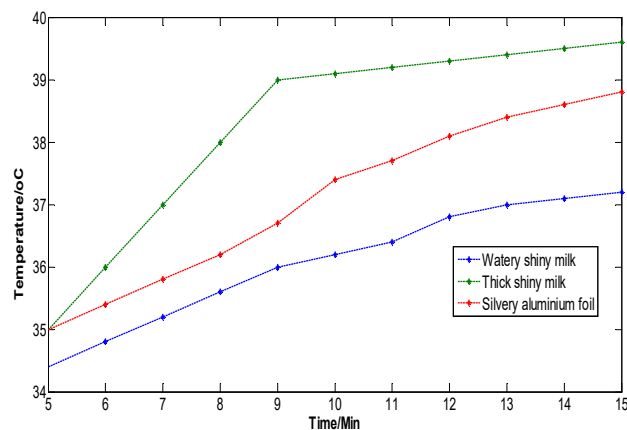**Figure-8:** Temperature-Time graph of Black coal tar, Black aluminium foil and Black liquor soap.

Figure-9: Temperature-Time graph of Watery shiny milk, Thick shiny milk and Silvery aluminum foil.
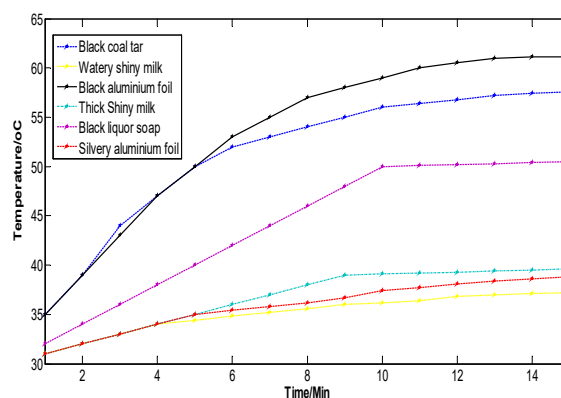

Figure-10: Temperature-Time graph of Black coal tar, Black aluminium foil, Black liquor soap, Shiny watery milk, Thick shiny milk and Silvery aluminium foil.

The experimental and calculated temperature distribution for slab with distributed heat sources are presented in Figure-4. From equation (22) given by experimental and theoretical results which are in good agreement. These results provide novel method to verify blackbody and its grade. In Figures-5 and 6, the temperature rate of absorption of radiations by black, silvery aluminium foils and black coal tar, thick shiny milk were all plotted as a function of time respectively. It is observed that for every one minute the curve of black surface/liquid rise higher and faster than that of silvery surface/liquid. These behaviours are not strange because black surfaces/liquids absorb radiations more than silvery surfaces/liquids.

It is also observed in Figure-7 that the temperature of black liquor soap rises proportionally with time from 1 to 10 minutes and maintain constant temperature at 50℃. However, the temperature of shiny watery milk rises up 38℃. Comparatively speaking black liquor soap absorbs more radiations than shiny watery milk. Figure 8 shows temperature-time graph for all black surfaces/liquids. It can be seen that, while the initial

temperature of both black coal tar and black aluminium foil are the same (35℃), black aluminium foil has greater heat absorption rate (64℃) with respect to time, followed by black coal tar (56℃) and then black liquor soap with (50℃). These results are expected as the foil is black solid and coal tar is thicker than liquor soap. Hence, amongst the black body samples, heat absorption and less radiation are more black solids than other black liquids.

The temperature-time graph for all silvery surfaces/liquids are shown in Figure-9. Results obtained in this figure are quite interesting and somewhat different from those in Figure 8. Thick shiny milk absorbs radiation at greater rate compared to silvery aluminium foil that reflect part of the radiation. On the other hand, watery shiny milk which is lighter reflect more of radiation and hence has less absorption powers.

Figure-10 shows the temperature rates for all black surfaces/ liquids and all silvery surfaces/liquids as a function of time. It is evidently shown that black surfaces absorb radiation at greater rate compared to silvery surfaces. Hence, black surfaces are good absorbers of radiations and good emitters of radiations while silvery surfaces are poor emitters of radiations and poor absorbers of radiations.

Conclusion

Absorption of radiation by black surfaces and silvery surfaces was carried out using several material samples of black and silvery surfaces/liquids. An investigation of our material samples using temperature sensors reveals that sharp increase in radiation are more pronounced on black surfaces/liquids than that of silvery surfaces/ liquids. The solutions of the material samples models were implemented using MALAB software and later exported to Microsoft word for comparism and analysis. The geometrical configuration was greatly altered as the power radiated from rear surfaces were measured by sensors as different material samples are taken into account with respect to time. We investigated theoretically that for an evacuated container, the thermal energy transfer is solely due to radiation as the vacuum is kept between two spheres while for a non-evacuated container, an extra heat transfer occurs due to the air's thermal conductance if the spheres separation contains air. The temperature distribution in presence of heat source was calculated and the result is in good agreement with the experimental results.

The results of the rate of absorption of radiation by the black surfaces and silvery surfaces for different material samples were compared. These results reveal that black surfaces absorb radiation at greater rate as compared to silvery surfaces with respect to time. Finally, we draw our conclusion by considering the fact from results that black surfaces are good absorbers of radiation while silvery surfaces are poor absorbers of radiation. Since good absorbers are also good emitters of radiation and that poor absorbers are also poor emitters of radiation, hence, black surfaces are also good emitters of radiation and silvery surfaces are poor emitters of radiation.

References

1. Nils D., Mariana D. and Leonardo G. (2011). Photon Gas in Equilibrium in Introductory Statistical thermodynamics. *Science Direct Publishers*, 2nd ed., 301-311.

2. Otor D.A., Echi I.M. and Amah A.N. (2018). Computational Study of Nonlinear Modulation of Wave Propagation in Model Media. *Research Journal of Physical Sciences*, 6(2), 9-20.

3. Otor D.A., Echi I.M. and Amah A.N. (2017). Nonlinear Modulation of Wave Propagation in Spherical Shell Model and Modified Zhang Model Using Free Space Model as a Bench-Mark. *Journal of Natural Sciences Research*, 7(3), 15-28.

4. Kasimir B., Tero S. and Ari T.F. (2015). Blackbody Aperture Radiation: Effect of Cavity Wall. *Physical Review Letter A,* 91: 063805.

5. Mahmoud Y., Massoud A. and Mickel N. (2005). Black body Radiation, Engineering Thermal Fluid; Thermodynamics Fluid Mechanics and Heat Transfer. *springer,* 41, 537.

6. Yamada Y. and Ishii J. (2015). Toward Reliable Industrial Radiation Thermometry. *International Journal of Thermophysics*, 36(5), 1699-1712.

7. Hagart-Alexander C. (2010). Temperature Measurement in Instrumentation Reference Book. *Science Direct Publishers*, 4th ed., 269-326.

8. Weisstein R., and Eric W. (2013). Eric weissteins world of physics. *Wolfram research,* 9(9), 596.

9. Yao K.A. and Curtis W.K (2000). Improved oxidation resistance of high emissivity coating on fibrous ceramic for reversible space system. *Academic press*, 9(73), 60-81.

10. Heather J. Peter P.K. and Hooked R. (2016). Infrared transmission of the atmosphere. *U.S naval research laboratory,* 2(2), 562.

11. Kwan- Hong W. Guenter J. (2003). Elements of cloud physics. *The university of Chicago press,* 3rd ed., pp 51-76.

12. Yang X. and Wei B. (2016). Exact Research on the Theory of the Blackbody Thermal Radiation. *Sci. Rep.*, 6, 37214.

13. Rocchii D. (2015). Earth Observation for Ecosystems Monitoring in Space and Time: A special Issue in Remote Sensing. *Remote Sensing,* 7, 8102-8106.

14. Chrzanowski K. (2013). Review of Night Vision Technology. *Opto-Electronic Review*, 21, 153-181.

15. Chen G.S., Lu W.Q., Cai R.H., and Ding, X.H. (2004). Research of Definitive Range of the Light Wavelength on Heat Radiation for Blackbody. *College Physics*, 23, 58-60.

16. Chen G.S., Lu W.Q., Cai R.H. and Ding, X.H. (2004). The Light Wavelength Equation of Inflexion in Planck Function. *Guangxi Sciences*, 11, 175-176.

17. Jubu, P. R., Otor, D. A. and Muttaka, U. (2018). Determination of the Thermal Properties of Groundnut Shell Particles Reinforced Polymer Composite. *IOSR-Journal of applied Physics (IOSR-JAP)*, 10(5), Version II, 51-57.

18. Planck M. (1914). Theory of Heat Radiation. *Blackiston's Son and Company*, 2nd ed., 450-470.

19. Lienhard J.H. (2000). Introduction to Engineering Heat Transfer in Fundamental of Heat Transfer. *Prentice-Hall Publishers*, 3rd ed., 34-36.